Scattering of Light by Light in Plasmas

D. F. DuBois
Hughes Research Laboratories, Malibu, California

AND

V. Gilinsky
The Rand Corporation, Santa Monica, California
(Received 2 March 1964)

A quantum-mechanical calculation of the scattering rate of light by light in the polarizable medium of a plasma is carried out. It is shown that if the frequency ω_0 of the incident light is much greater than the electron plasma frequency ω_p, the $\rho\mathbf{A}^2$ term in the nonrelativistic Hamiltonian coupling the radiation to matter dominates the $\mathbf{j}\cdot\mathbf{A}$ interaction, provided the frequency shifts $\Delta\omega$ satisfy $\Delta\omega\ll\omega_0$. In this approximation, the scattering amplitude is proportional to the Green's function for electron-density fluctuations (which reduces to the electron-density correlation function in the classical limit). This leads to an expression for the differential scattering rate which is formally exact to all orders in the interparticle interactions. The spectrum of the scattered light in this approximation has resonances at the collective modes of the plasma if $\omega_0/c\ll k_D$, the Debye wave number. The total scattering rate is estimated in the collisionless (random-phase) approximation. Under the conditions of this calculation, rather high plasma densities and temperatures are required to obtain a detectable rate.

I. INTRODUCTION

THE development of the optical laser has stimulated interest in nonlinear electromagnetic interactions. A polarizable medium such as a plasma or even the vacuum provides the nonlinear interaction making possible the scattering of one photon by another. The process can be described as the absorption of the radiation by a virtual density fluctuation of the medium (virtual pair production in the vacuum case) which is in turn de-excited by producing new radiation. An energy of mc^2 is necessary to appreciably polarize the vacuum so that the resulting cross section is of order[1] $r_0^2\alpha^2(\hbar\omega/mc^2)^6$ for low energies and is extremely small at optical frequencies. A plasma, on the other hand, is very easy to polarize and one expects a much larger cross section. This paper is concerned with a quantum-mechanical calculation of this cross section. The most interesting features of the result are the relatively large and probably observable scattering rate using typical laser parameters and hot, dense plasmas and the resonances in the scattered spectrum at the collective modes of a plasma.

Since we use a nonrelativistic Hamiltonian, the interaction of the radiation with matter consists of a $\mathbf{j}\cdot\mathbf{A}$ term ($\mathbf{j}$ is the current density operator and $\mathbf{A}$ is the vector potential of the transverse radiation field) and a ρA^2 term (ρ is the charge-density operator). The key approximation in this calculation is that the $\mathbf{j}\cdot\mathbf{A}$ interaction can be neglected compared with the $\rho\mathbf{A}^2$ interaction if the frequency ω_0 of the incoming light is much greater than the plasma frequency ω_p provided the frequency shifts in scattering are much less than ω_0. In Sec. II it is shown that the S-matrix element as calculated in this approximation is proportional to the density-density Green's function of the plasma. The conditions for the validity of this approximation are discussed in Sec. III. In Sec. IV the kinematics for this process are analyzed, a formally exact formula (in the $\rho\mathbf{A}^2$ approximation) for the differential scattering rate and an estimate of the total scattering rate for this process in the collisionless approximation are given.

II. SCATTERING AMPLITUDE IN HIGH-FREQUENCY LIMIT

Our treatment will be based on the nonrelativistic Hamiltonian for matter and radiation which can be written

$$H=H_m+H_R+H_{\text{int}}, \tag{2.1}$$

where H_m is the complete Hamiltonian of the interacting many-particle system, H_R represents the free radiation field and

$$H_{\text{int}}=H_1+H_2, \tag{2.2}$$

$$H_1=-\frac{1}{c}\int d^3x\mathbf{j}(\mathbf{x},t)\cdot\mathbf{A}(\mathbf{x},t), \tag{2.3}$$

$$H_2=\sum_s\frac{e^2Z_s^2}{2m_sc^2}\int d^3xn_s(\mathbf{x},t)\mathbf{A}(\mathbf{x},t)\cdot\mathbf{A}(\mathbf{x},t), \tag{2.4}$$

where $\mathbf{j}(\mathbf{x},t)$ is the total current-density operator (proportional to e) for the matter (in the absence of radiation), $n_s(\mathbf{x},t)$ is the number-density operator for particles of species s with mass m_s and charge ez_s. $\mathbf{A}(\mathbf{x},t)$ is the transverse vector-potential operator for the electromagnetic field which we treat in the Coulomb gauge ($\nabla\cdot\mathbf{A}=0$). Because of the mass dependence of (2.3) we need only consider the interaction with the electron

[1] A comprehensive summary of the vacuum theory is given by J. M. Jauch and F. Rohrlich, *The Theory of Photons and Electrons* (Addison Wesley Publishing Company, Inc., Reading, Massachusetts, 1955), Chap. 13. Here $r_0=e^2/mc^2$ is the classical electron radius.

density to terms of order m_e/m_i. Similarly, only the electron component of the current is important in this case.

We wish to calculate the S-matrix element between an initial state of two photons $(\hat{e}_1,k_1;\,\hat{e}_2,k_2)$ and a final state of two photons $(\hat{e}_2,k_3;\,\hat{e}_4,k_4)$. The Dyson-Wick expansion in the interaction picture of the matter-field interaction (which is the Heisenberg picture of the interacting system without radiation field) yields the following terms of fourth order in the vector potential:

$$S^{(2)}=\left(-\frac{i}{\hbar}\right)^2\frac{1}{2!}\left(\frac{e^2}{2mc^2}\right)^2\int d^4x_1\int d^4x_2 \times\langle Tn_e(1)n_e(2)\rangle\cdot N[\mathbf{A}^2(1)\mathbf{A}^2(2)]\,, \quad (2.5)$$

$$S^{(3)}=3\left(-\frac{i}{\hbar}\right)^3\frac{1}{3!}\left(\frac{e^2}{2mc^4}\right)\int d^4x_1\int d^4x_2\int d^4x_3 \times\langle Tn_e(1)j_\mu(2)j_\nu(3)\rangle\cdot N[\mathbf{A}^2(1)A_\mu(2)A_\nu(3)]\,, \quad (2.6)$$

$$S^{(4)}=\left(-\frac{i}{\hbar}\right)^4\frac{1}{4!c^4}\int d^4x_1\int d^4x_2\int d^4x_3\int d^4x_4 \times\langle Tj_\mu(1)j_\nu(2)j_\sigma(3)j_\rho(4)\rangle \cdot N[A_\mu(1)A_\nu(2)A_\sigma(3)A_\rho(4)]\,. \quad (2.7)$$

Here T is Wick's chronological operator and N is the normal product. Of these contributions only $S^{(2)}$ makes an important contribution if ω_1 and ω_2 are high frequencies compared, say, to the plasma frequency. This is a crucial argument in simplifying the calculation. The argument for this approximation will be given in Sec. III following the calculation of the $S^{(2)}$ contribution.

The $S^{(2)}$ matrix element for this problem is

$$\langle\mathbf{k}_3\hat{\mathbf{e}}_3;\,\mathbf{k}_4\hat{\mathbf{e}}_4|S^{(2)}|\mathbf{k}_1\hat{\mathbf{e}}_1;\,\mathbf{k}_2\hat{\mathbf{e}}_2\rangle =\left(\frac{e^2}{mc^2}\right)^2\frac{(4\pi)^2c^4V_0^{-2}(n_1n_2)^{1/2}}{(16\omega_1\omega_2\omega_3\omega_4)^{1/2}} \times e_1{}^\mu e_2{}^\nu e_3{}^\sigma e_4{}^\rho G_{\mu\nu\sigma\rho}{}^{(2)}(k_1k_2k_3k_4)(2\pi)^4 \times\delta^3(\mathbf{k}_1+\mathbf{k}_2-\mathbf{k}_3-\mathbf{k}_4)\delta(\omega_1+\omega_2-\omega_3-\omega_4)\,. \quad (2.8)$$

The electromagnetic field is normalized to n_1 and n_2 photons in the incident beams in a volume V_0 corresponding to the interaction volume of the two laser beams and we have used the notation $k_1=(\mathbf{k}_1,\omega_1)$ and $\omega_1=|\mathbf{k}_1|c$ where

$$e_1{}^\mu e_2{}^\nu e_3{}^\sigma e_4{}^\rho G_{\mu\nu\sigma\rho}{}^{(2)}(k_1k_2k_3k_4) =\hbar\{(\hat{e}_1\cdot\hat{e}_2)(\hat{e}_3\cdot\hat{e}_4)\Pi_{ee}(k_1+k_2) +(\hat{e}_1\cdot\hat{e}_3)(\hat{e}_2\cdot\hat{e}_4)\Pi_{ee}(k_3-k_1) +(\hat{e}_1\cdot\hat{e}_4)(\hat{e}_2\cdot\hat{e}_3)\Pi_{ee}(k_4-k_1)\}\,. \quad (2.9)$$

Here

$$\Pi_{ee}(k)=\int d^4(x_1-x_2)e^{ik\cdot(x_1-x_2)}\Pi_{ee}(1,2)\,, \quad (2.10)$$

$$\Pi_{ee}(1,2)=\hbar^{-1}\langle Tn_e(1)n_e(2)\rangle\,.$$

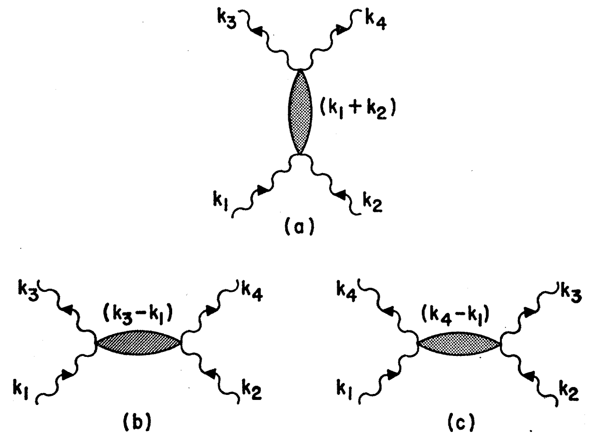

FIG. 1. The three basic contributions to the scattering amplitude in the $\rho\mathbf{A}^2$ or high-frequency approximation. The wavy lines represent the photons and the shaded bubble represents the electron density Green's function $\Pi_{ee}(k)$ which carries the momentum and energy denoted in parenthesis $(k)=(\mathbf{k},\omega)$. a, b, and c refer, respectively, to the three terms in the amplitude of Eq. (2.9).

The brackets $\langle\cdots\rangle$ denote the average in the equilibrium ensemble of the matter. $\Pi_{ee}(1,2)$ is the Green's function for electron-density fluctuations. A useful graphical representation of this amplitude is given in Fig. 1. The shaded bubble represents the propagation of a density fluctuation in the system. For certain values of the k's the resonances of Π_{ee} will contribute and we can describe the scattering process as involving an exchange of plasmons. To take the classical limit of this result we express Π_{ee} in terms of the retarded commutator[2]

$$\Pi_{ee}{}^+(1,2)=\hbar^{-1}\eta(t_1-t_2)\langle[n_e(1),n_e(2)]_-\rangle\,. \quad (2.11)$$

The transforms are related by[2]

$$\Pi_{ee}(\mathbf{k},\omega)=\mathrm{Re}\Pi_{ee}{}^+(\mathbf{k},\omega) \times i\coth\tfrac{1}{2}\beta\hbar\omega\,\mathrm{Im}\Pi_{ee}{}^+(k,\omega)\,. \quad (2.12)$$

So

$$\lim_{\hbar\to 0}\hbar\Pi_{ee}(\mathbf{k},\omega)=2i(\mathrm{Im}\Pi_{ee}{}^+(\mathbf{k},\omega)/\beta\omega)\,. \quad (2.13)$$

In the classical limit only $\mathrm{Im}\Pi_{ee}{}^+$ occurs which describes real density fluctuations (in distinction to $\mathrm{Re}\Pi_{ee}{}^+$ which describes virtual processes). Therefore, this amplitude involves a real intermediate state and is closely related to the cross section for incoherent scattering.[3] (The function $\Pi_{ee}{}^+$ differs by a factor $4\pi e^2$ from the function $\Pi_e{}^+$ defined in Ref. 3.) The functions $\Pi_{ee}{}^+$ can be related to the partial conductivities of the system and the longitudinal dielectric function as shown in Ref. 3. Here we consider only a classical plasma in the random-

---

[2] A. A. Abrikosov, L. P. Gorkov, and I. E. Dzyaloshinskii, *Methods of Quantum Field Theory in Statistical Mechanics* (Prentice-Hall Inc., Englewood Cliffs, New Jersey, 1963).

[3] D. F. DuBois and V. Gilinsky, Phys. Rev. **133**, A1308 and A1317 (1964), parts I and II.

phase approximation (RPA)[3]:

$$\frac{4\pi e^2}{k_D^2}\operatorname{Im}\Pi_{ee}^+(\mathbf{k},\omega)=\left(\frac{\pi}{2}\right)^{1/2}\frac{\omega}{k}e^{-\frac{1}{2}(\omega/k)^2}\left|1-\frac{Q_0^+(\omega/k)}{k^2\epsilon_L^+(\mathbf{k},\omega)}\right|^2+\left(\frac{\pi}{2}\right)^{1/2}\frac{\omega}{\alpha k}e^{-\frac{1}{2}(\omega/\alpha k)^2}\left|\frac{Q_0^+(\omega/k)}{k^2\epsilon_L^+(\mathbf{k}\omega)}\right|^2,\quad(2.14)$$

where k and ω are measured in units of the Debye wave number $k_D=(4\pi e^2 n\beta)^{1/2}$ and ω_p, and

$$\epsilon_L^+(\mathbf{k},\omega)=1+k^{-2}Q_0^+(\omega/k)+k^{-2}Q_0^+(\omega/\alpha k)\,,\quad(2.15)$$

$$\alpha=(m_e/m_i)^{1/2}\,,\quad(2.16)$$

$$Q_0^+(\omega/k)=1-\frac{\omega}{k}e^{-\frac{1}{2}(\omega/k)^2}\int_0^{\omega/k}dte^{\frac{1}{2}t}+i\left(\frac{\pi}{2}\right)^{1/2}\frac{\omega}{k}e^{-\frac{1}{2}(\omega/k)^2}.\quad(2.17)$$

III. HIGH-FREQUENCY APPROXIMATION

Next, we consider the contributions of $S^{(3)}$ and $S^{(4)}$ to the scattering amplitude. It is easily shown that the total amplitude including these contributions is given by (2.8) by adding to $G_{\mu\nu\sigma\rho}^{(2)}(k_1k_2;k_3k_4)$ the terms $G_{\mu\nu\sigma\rho}^{(3)}$ and $G_{\mu\nu\sigma\rho}^{(4)}$. The $S^{(3)}$ contribution is

$$\begin{aligned}&\hat{e}_1^\mu\hat{e}_2^\nu\hat{e}_3^\sigma\hat{e}_4^\rho G_{\mu\nu\sigma\rho}^{(3)}(k_1,k_2;k_3,k_4)\\&=\hat{e}_1^\mu\hat{e}_2^\nu\hat{e}_3^\sigma\hat{e}_4^\rho\hbar(m/e^2)\\&\times\{\delta_{\sigma\rho}R_{\mu\nu}(k_1,k_2;k_3+k_4)+\delta_{\nu\rho}R_{\mu\sigma}(k_1,k_3;k_4-k_2)\\&+\delta_{\nu\sigma}R_{\mu\rho}(k_1,k_4;k_3-k_2)\}\\&+(3\text{ similar terms with }1\rightleftharpoons3;\,2\rightleftharpoons4)\,.\quad(3.1)\end{aligned}$$

Here

$$R_{\mu\nu}(k_1,k_3;k)\equiv\hbar^{-2}\int_{-\infty}^{\infty}dt_1\int_{-\infty}^{\infty}dt_3e^{i\omega_1t_1}e^{-i\omega_3t_3}\times\langle Tj_\mu(\mathbf{k}_1,t_1)j_\nu(\mathbf{k}_3,t_3)\rho(k,0)\rangle\,,\quad(3.2)$$

where the Heisenberg operator $j_\mu(\mathbf{k},t)$ is defined by

$$j_\mu(\mathbf{k},t)=\int d^3xe^{i\mathbf{k}\cdot\mathbf{x}}j_\mu(\mathbf{x},t)\,,\quad(3.3)$$

with a similar definition for $\rho(k,0)$.

The $S^{(4)}$ contribution is

$$\begin{aligned}&\hat{e}_1^\mu\hat{e}_2^\nu\hat{e}_3^\sigma\hat{e}_4^\rho G_{\mu\nu\sigma\rho}^{(4)}(k_1,k_2;k_3,k_4)\\&=\hat{e}_1^\mu\hat{e}_2^\nu\hat{e}_3^\sigma\hat{e}_4^\rho\hbar(m/e^2)^2\{T_{\mu\nu\sigma\rho}(k_1,k_2;k_3,k_4)\\&+T_{\mu\sigma\nu\rho}(k_1,k_3;k_2,k_4)+T_{\mu\rho\nu\sigma}(k_1,k_4;k_2,k_3)\}\\&+(3\text{ terms with }1\rightleftharpoons3;\,2\rightleftharpoons4)\,,\quad(3.4)\end{aligned}$$

where here

$$T_{\mu\nu\sigma\rho}(k_1,k_2;k_3,k_4)=\hbar^{-3}\int_{-\infty}^{\infty}dt_1\int_{-\infty}^{\infty}dt_2\int_{-\infty}^{\infty}dt_3e^{i\omega_1t_1}e^{i\omega_2t_2}e^{-i\omega_3t_3}\times\langle Tj_\mu(\mathbf{k}_1,t_1)j_\nu(\mathbf{k}_2,t_2)j_\sigma(\mathbf{k}_3,t_3)j_\rho(\mathbf{k}_4,0)\rangle\,.\quad(3.5)$$

An exact evaluation of these contributions is difficult to carry out beyond the RPA for reasons to be discussed. However, the criterion for the neglect of these contributions can be established by general physical arguments.

First, let us backtrack a moment and notice that in (2.9), the last two terms in the amplitude depend only on the frequency *differences* $\omega_1-\omega_3$, $\omega_2-\omega_4$, whereas the first term depends on the sum $\omega_1+\omega_2$. If we let ω_1 and ω_2 become large compared with ω_p while keeping $|\omega_1-\omega_3|$, $|\omega_2-\omega_4|\lesssim\omega_1$, ω_2 the term depending on $\omega_1+\omega_2$ becomes negligible in comparison with the terms depending on the frequency differences. This follows from the *exact* asymptotic form of Π_{ee}:

$$4\pi e^2\Pi_{ee}(\mathbf{k},\omega)\underset{\omega\to\infty}{\longrightarrow}\langle[j_\mu(\mathbf{k},0),\rho(-\mathbf{k},0)]\rangle/\omega^2=k^2\omega_p^2/\omega^2.$$

This can be seen explicitly for Π_{ee} in the RPA as given in (2.14).

Similarly, the functions $R_{\mu\nu}$ and $T_{\mu\nu\sigma\rho}$ depend on the individual frequencies ω_1, ω_2, ω_3 and not only on the frequency differences. For any physically realizable functions of the time variables in (3.2) and (3.5) it follows from the general properties of Fourier transforms

$$\lim_{\omega_1\to\infty,\,\omega_3\to\infty}R_{\mu\nu}(\mathbf{k}_1,\omega_1;\mathbf{k}_3,\omega_3;\mathbf{k})=0\,,\quad(3.7)$$

$$\lim_{\omega_1,\omega_2,\omega_3\to\infty}R_{\mu\nu\sigma\rho}(\mathbf{k}_1,\omega_1;\mathbf{k}_2,\omega_2;\mathbf{k}_3,\omega_3;\mathbf{k}_4)=0\,.\quad(3.8)$$

This statement applies if the time functions in the integrands of (3.2) and (3.5) have no singular behavior worse than step functions. To define the transforms in (3.2) and (3.5) we must, as usual in S-matrix theory insert the convergence factors $e^{-|\epsilon|t_i}$ for each time variable t_i where the limit $\epsilon\to0+$ is ultimately to be taken. The asymptotic limits can actually be carried out formally by expanding the integrands about $t_i=0$. This leads to a result for $R_{\mu\nu}$, for example, involving a series of terms involving inverse powers of ω_1 and ω_3 with numerators which are averages of products of $\rho(k,0)$ with various time derivatives (including the zeroth) of the current operators. The explicit results are too complicated to give here.

It is clear then that for *sufficiently* high ω_1 and ω_2, i.e., ω_1, $\omega_2\gg\omega_m$, the contributions from $S^{(3)}$ and $S^{(4)}$ can be neglected relative to those of $S^{(2)}$ provided we restrict $|\omega_1-\omega_3|$, $|\omega_2-\omega_4|\ll\omega_1$. It remains to be shown what scale of frequencies is involved. Of the parameters of the plasma e^2, n, m, M, T the only frequencies that can be formed are the plasma frequency $\omega_p=(4\pi e^2n/m)^{1/2}$ or ω_p times some function of the dimensionless parameters $\lambda=k_D^3/n$, $\alpha=(m/M)^{1/2}$. If we include the parameters k_i describing the radiation, we can also form the frequencies $k_iv_e=k_i(kT/m)^{1/2}=(k_i/k_D)\omega_p$ or some combination of λ and α times these. If $\lambda\ll1$ and $k_i<k_D$, the highest frequency of significance in plasma physics is ω_p. Therefore, a reasonable conservative estimate is to take $\omega_m=\omega_p$. Since we must have ω_1, $\omega_2\gg\omega_p$ for the inci-

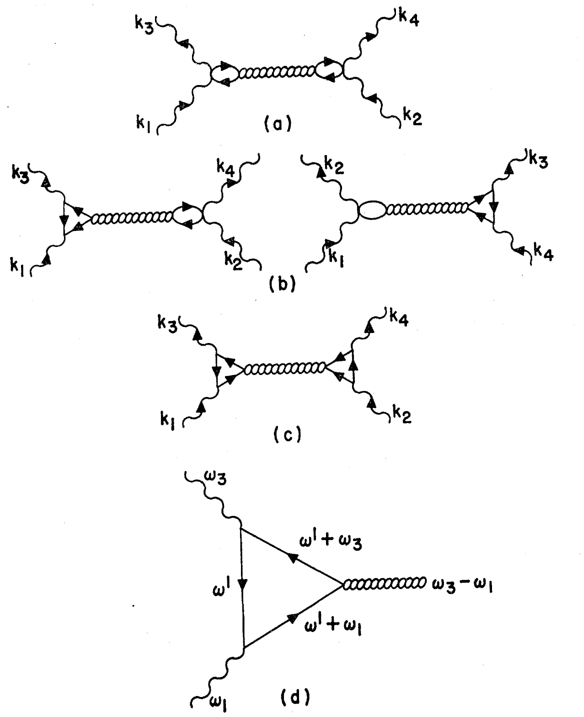

FIG. 2. Diagrams for resonant processes in the collisionless (RPA) approximation; (a) contribution to $G_{\mu\nu\sigma\rho}^{(2)}$; (b) contribution to $G_{\mu\nu\sigma\rho}^{(3)}$; (c) contribution to $G_{\mu\nu\sigma\rho}^{(4)}$. The total amplitude is obtained by including all permutations of the photon vertices which lead from the same initial to the same final state. The braided line represents the dynamically screened Coulomb interaction. (d) Detail of the triangular vertices.

dent light to penetrate the plasma, this is not a serious restriction.

More detailed arguments (see Ref. 3 and below) show that actually, ω_m is of the order of the electron-ion collision Γ_{ei} frequency if $v_e \ll c$,

$$\Gamma_{ei} = \lambda C_1 \omega_p \ln(C_2 \lambda^{-1}), \tag{3.9}$$

where C_1 and C_2 are constants. This can be made plausible, for example, by expanding the integrand (3.2) around $t_1 = 0$ and $t_3 = 0$ to obtain the asymptotic form for large ω_1, ω_3. It is easily shown that for the transverse components (i.e., $e_1^{\mu} e_3^{\nu} R_{\mu\nu}$) the leading terms involving $j_\mu(k_1,0)$ and $j_\nu(k_3,0)$ vanish leaving only higher order terms involving time derivatives of $j_\mu(k_1,t_1)$ and $j_\nu(k_3,t_3)$ at $t=0$ and $t_3=0$. The frequency associated with the time rate of change of the current is the electron-ion collision frequency.

From these arguments we can abstract the general statement that the $\mathbf{j}\cdot\mathbf{A}$ interaction can be neglected if the frequency of the incident light in a scattering problem is so high that in one period of the light the induced currents in the system cannot change appreciably. The currents in a plasma ($kv_e \ll \omega$) can change appreciably only in a time of order Γ_{ei}^{-1}. For bound electrons in an atom the current changes appreciably in a time of the order of $\hbar(E_n - E_0)^{-1}$ where $E_n - E_0$ are the excitation energies of the atom. Thus, for $\hbar\omega \ll E_n - E_0$ we have the well-known result that the $\mathbf{j}\cdot\mathbf{A}$ terms and the $\rho\mathbf{A}^2$ are of comparable magnitude with an important cancellation leading to Rayleigh scattering. On the other hand, for $\hbar\omega \gg E_n - E_0$, the $\mathbf{j}\cdot\mathbf{A}$ terms are negligible compared to $\rho\mathbf{A}^2$ which give rise to Thompson scattering.

Finally, let us discuss these results in terms of the diagram expansion of the amplitudes $R_{\mu\nu}$ and $T_{\mu\nu\sigma\rho}$. Here we must make use of the theory of temperature Green's functions[2,4,5] in which, for example, we go over to imaginary temperatures $\beta = i\tau$ so in the averages we have

$$\langle \cdots \rangle = \mathrm{Tr}(e^{-i\tau H} \cdots). \tag{3.10}$$

This allows us to impose periodicity conditions in time on the imaginary temperature Green's functions[4] $\tilde{R}_{\mu\nu}$ and $\tilde{T}_{\mu\nu\sigma\rho}$ and we can then use Feynman diagram methods as discussed in Ref. 5.

In Fig. 2(a) we draw a contribution to $G_{\mu\nu\sigma\rho}^{(2)}$ in the collisionless approximation (RPA). Here the braided line represents the dynamically screened Coulomb interaction[5] which has resonances at the collective modes of the plasma. In Figs. 2(b) and 2(c) we draw the analogous contributions from $G_{\mu\nu\sigma\rho}^{(3)}$ and $G_{\mu\nu\sigma\rho}^{(4)}$, respectively. The double photon or $\rho\mathbf{A}^2$ vertex in Fig. 2(a) transfers the difference frequency $\omega_1 - \omega_3$ to the simple polarization loop. The single photon or $\mathbf{j}\cdot\mathbf{A}$ vertices in the triangular loops in Figs. 2(b) and 2(c), however, depend on the separate frequencies ω_1, ω_2 and so introduce large energy denominators for ω_1, $\omega_2 \gg \omega_p$ into these terms.

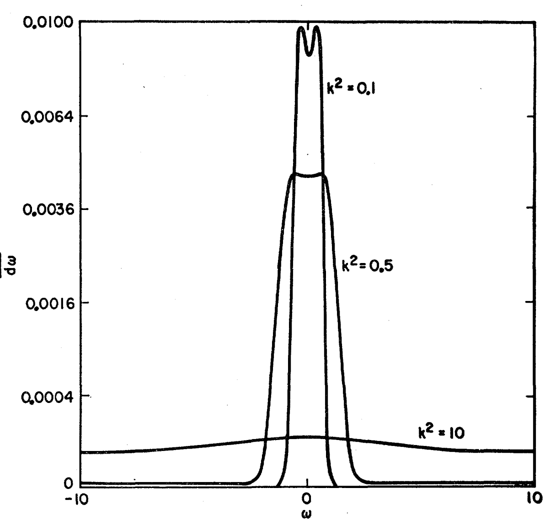

FIG. 3. The spectral shape of the scattered light. Here we plot $d\Gamma/d\omega$ in the RPA versus $\omega = (\omega_0 - \omega_3)/\omega_p$ various values of $k = k^1 = |\mathbf{k}_1 - \mathbf{k}_3| k_D^{-1}$. The vertical scale is arbitrary. The ω scale is normalized to αk. The relatively weak resonances at $\omega = \pm 1$ are not shown on this graph.

[4] P. Martin and J. Schwinger, Phys. Rev. **115**, 1342 (1959).
[5] D. F. DuBois, V. Gilinsky, and M. Kivelson, Phys. Rev. **129**, 2376 (1963).

For small k and ω (in plasma units) we can find the explicit contribution of the $\mathbf{j}\cdot\mathbf{A}$ interaction by appealing to a type of Ward identity. The amplitude for the triangular loop in Fig. 2(d) is given by [remembering $\mathbf{k}_3=\mathbf{k}_1+\mathbf{k}$, $\omega_3=\omega_1+\omega$ and identifying p_0 with ω^1 in Fig. 2(d)]

$$e_1^\mu e_3^\nu \tilde{\Delta}_{\mu\nu}^0(\mathbf{k}_1,k_{10};\mathbf{k},\omega)=-\frac{4\pi e^2}{m^2}\int\frac{d^3p}{(2\pi)^3}(\mathbf{p}\cdot\hat{e}_1)(\mathbf{p}+\mathbf{k}_1)\cdot\hat{e}_2$$
$$\times\frac{1}{\beta}\sum_{p_0}\frac{i}{p_0-\xi_\mathbf{p}}\frac{i}{p_0+k_{10}-\xi_{\mathbf{p+k}}}\frac{i}{p_0+k_0-\xi_{\mathbf{p+k}}}$$
$$+(\text{similar term with } k_{10}\to -k_{10},\ \mathbf{k}_1\to-\mathbf{k}_1)\quad(3.11)$$

using here the rules of Ref. 5. The transverse photon self-energy part as discussed in Ref. 6. Equation (4.41) is given by

$$\tilde{Q}_T^0(\mathbf{k},k_0)=\frac{4\pi e^2}{m^2}\int\frac{d^3p}{(2\pi)^3}(\mathbf{p}\cdot\hat{e}_1)(\mathbf{p}+\mathbf{k}_1)\cdot\hat{e}_2$$
$$\times\sum_{p_0}\frac{i}{p_0-\xi_\mathbf{p}}\frac{i}{p_0+k_0-\xi_{\mathbf{p+k}}}.\quad(3.12)$$

This is represented by a simple polarization loop. Were we generalized slightly from Ref. 6 by taking the polarizations of the incident and outgoing photons to be different.

Next, expand $\tilde{\Delta}_{\mu\nu}^0$ in powers of $\mathbf{k}$ and k_0 (in plasma units)

$$e_1^\mu e_3^\nu\tilde{\Delta}_{\mu\nu}^0(\mathbf{k}_1,k_{10};\mathbf{k},k_0)=e_1^\mu e_3^\nu\tilde{\Delta}_{\mu\nu}^0(\mathbf{k}_1,k_{10};0,0)+O(k_0,\mathbf{k}).\quad(3.13)$$

we can then use a Ward identity of the form

$$\frac{1}{(p_0-\xi_\mathbf{p})^2}=-\frac{\partial}{\partial\mu}\frac{1}{p_0-\xi_\mathbf{p}}=-\frac{\partial}{\partial\mu}\frac{1}{[p_0-(\mathbf{p}^2/2m)+\mu]}\quad(3.14)$$

(where μ is the chemical potential) to connect[7] $\tilde{\Delta}_{\mu\nu}^0(\mathbf{k}_1,k_{10};0,0)$ with $Q_T^0(\mathbf{k}_1,k_{10})$:

$$e_1^\mu e_3^\nu\tilde{\Delta}_{\mu\nu}(\mathbf{k}_1,k_{10};0,0)=i(\partial/\partial\mu)\tilde{Q}_T(\mathbf{k}_1,k_{10}).\quad(3.15)$$

This is useful because the properties of $\tilde{Q}_T$ have been given in previous work. More importantly, it is not hard to see that this identity applies to the fully corrected loops as signified by the omission of the zero superscripts in (3.15). We may include all possible self-energy and vertex corrections in the loops for Q_T and $\Delta_{\mu\nu}$. Differentiation with respect to μ is equivalent to attaching one zero momentum, zero-frequency screened interaction line in all possible ways in the particles lines of $\tilde{Q}_T$ and is therefore equivalent to $e_1^\mu e_3^\nu\tilde{\Delta}_{\mu\nu}(\mathbf{k}_1,k_{10};0,0)$.

In order to use (3.15) in the present problem, we must be able to analytically continue the tilde functions of discrete energy variables k_{10} to obtain the Green's functions $Q_T(\mathbf{k}_1,\omega_1)$ and $\Delta_{\mu\nu}(\mathbf{k}_1,\omega_1;0,0)$ of the continuous variables ω_1. For the two point function $Q_T(\mathbf{k}_1,\omega_1)$ the procedure is well known.[2] We define a function $Q_T^+(\mathbf{k}_1,\omega_1)$ analytic in the upper half-plane by setting $k_{10}=\omega_1$ for values of ω_1 in this half-plane. Then for real ω_1

$$Q_T(\mathbf{k}_1,\omega_1)=\mathrm{Re}Q_T^+(\mathbf{k}_1,\omega_1)+i\coth\tfrac{1}{2}\beta\hbar\omega_1\,\mathrm{Im}Q_T^+(\mathbf{k}_1,\omega_1).\quad(3.16)$$

To our knowledge a comparable continuation procedure for three point functions such as $\Delta_{\mu\nu}(\mathbf{k}_1,\omega_1;\mathbf{k},\omega)$ is not known. We shall therefore assume that for $\Delta_{\mu\nu}(\mathbf{k}_1,\omega_1;0,0)$ the continuation procedure is the same as for $Q_T(\mathbf{k}_1,\omega_1)$. In the asymptotic limit this is probably valid. The analytic continuation procedure is a prescription for treating the poles of the denominators in $\Delta_{\mu\nu}(\mathbf{k}_1,\omega_1;0,0)$ by proper assignment of $\pm i\epsilon$'s. In the asymptotic limit in which ω_1 is much greater than any of the important states of the system this assignment is not important. For example, as $\omega_1\to\infty$ in (3.16) we see

$$Q_T(\mathbf{k}_1,\omega_1)\xrightarrow[\omega_1\to\infty]{}Q_T^+(\mathbf{k}_1,\omega_1).\quad(3.17)$$

Therefore, for large ω_1 we can write

$$e_1^\mu e_3^\nu\Delta_{\mu\nu}^+(\mathbf{k}_1,\omega_1;0,0)=i(\partial/\partial\mu)Q_T^+(\mathbf{k}_1,\omega_1).\quad(3.18)$$

From Refs. 5 and 6 it follows that[8] if $\lambda\ll1$, $k_1v_e\ll\omega_1$ $\omega_1\gg\Gamma_{ei}$

$$\frac{1}{\beta}\frac{\partial}{\partial\mu}Q_T^+(\mathbf{k}_1,\omega_1)=\tfrac{1}{3}(\hat{e}_1\cdot\hat{e}_3)\frac{k_1^2}{k_D^2}\frac{\omega_p^4}{\omega_1^2}+2i(\hat{e}_1\cdot\hat{e}_3)\frac{\omega_p^2}{\beta\hbar\omega_1^2}\Gamma_{ei}(1-e^{-\beta\hbar\omega_1}),\quad(3.19)$$

where Γ_{ei} is roughly as given in (3.9). An exact formula is given in Ref. 5. In this formula we have kept only the leading terms in the real and imaginary parts. The real part is contributed by Q_T^{0+}, i.e., the RPA [which has no imaginary part if $\omega_1=k_1c$ (see Ref. 6)] while the leading term in the imaginary part comes from the collision corrections to Q_T^+.

The expression for $\Delta_{\mu\nu}(k_1,\omega_1;0,0)$ obtained from (3.18)

---

[6] D. F. DuBois, V. Gilinsky, and M. Kivelson, Rand Corporation, Report RM-3224-AEC, August 1962 (unpublished).

[7] The limit $\omega\to0$, $k\to0$ is actually ambiguous. It is easily shown that the limit implied by (3.15) is $\omega\to0$, $k\to0$ with $\omega/k\to0$. Therefore, this limit applies near the acoustic ion resonance where $\omega/k\sim\alpha\ll1$.

[8] To derive this expression we note that the density n enters these expressions only via the chemical potentials μ_e and μ_i. In the limit of classical statistics considered here $\partial/\partial\mu_e=\partial/\partial\mu_i=n\beta\partial/\partial_n$. The expression for $4\pi\,\mathrm{Im}\sigma_T(\mathbf{k},\omega)=Q_T(\mathbf{k},\omega)\cdot\omega^{-1}$ given in Ref. 5, Eqs. (6.23) and (6.25) are proportional to n^2 and in the high-frequency limit $\omega\gg\omega_p$ [see Eq. (6.24)] this is the only density dependence and $\Gamma_{ei}(\omega)=\lambda\omega_p(6\sqrt{2}\pi^{3/2})^{-1}\ln(4e^{-C}/\beta\hbar\omega)$, where C is Euler's constant. We have also restored a factor $(\beta\hbar\omega)^{-1}(1-e^{-\beta\hbar\omega})$ which was taken to be 1 in Ref. 5 for the case $\beta\hbar\omega\ll1$.

and (3.19) is to be compared with the corresponding ρA^2 vertex which is $(1/m)Q_e^+(k,\omega)$ where $Q_e^+(k,\omega)$ is the complete electron polarization part defined in Refs. 3 and 4. In these references it is shown explicitly that in the collisionless approximation and in the collision dominated approximation that $Q_e^+(k,\omega)=k_D^2$ when $kv_e\gg\omega$. This limit appears to be generally valid. Since in this case $(1/m)Q_e^+=\beta\omega_p^2$ we see that the first term in (3.19) arising from the collisionless approximation can be neglected relative to $(1/m)Q_e^+$ provided $kT\ll mc^2$ (noting that $\omega_1=k_1c$). Likewise the second term or collision correction can be neglected provided $\omega_1>\omega_p\gg\Gamma_{ei}$.

The requirement $k_1<k_D$ discussed preceding (3.9) is unnecessarily restrictive as we see from the argument just given. Equation (3.19) is valid for all values of k_1 for which $k_1v_e\ll\omega_1=k_1c$. This is satisfied independent of k_1 as long as $k_BT\ll mc^2$. The argument above applies when $k=|k_1-k_3|\ll k_D$ for frequency shifts ω in the neighborhood of the collectively narrowed ion resonance and therefore the diagrams considered above dominate in this case.[3] In the case $k\gg k_D$, on the other hand, it is physically clear that the scattering must reduce to the scattering from independent free electrons, i.e., essentially to Thomson scattering. In this case it is well known that only the ρA^2 interaction contributes for frequencies such that $\hbar\omega_1$, $\hbar\omega_2\ll mc^2$.

We conclude then from these arguments that the ρA^2 interaction dominates the $\mathbf{j}\cdot\mathbf{A}$ interaction provided ω_1, $\omega_2>\omega_p$ while $|\omega_1-\omega_3|$, $|\omega_2-\omega_4|\ll\omega_1$, ω_2, and $kT\ll mc^2$. A more detailed study of these requirements in the vicinity of the plasma resonance is in progress. The general arguments made preceding (3.9) indicate that the same restrictions apply in this case. It is clear that the ρA^2 approximation is valid in the RPA if $k_BT\ll mc^2$.

IV. SCATTERING RATE AND KINEMATICS

The total scattering rate Γ is found from the amplitude using the well-known relation[1]

$$\Gamma=V_0(2\pi\hbar)^4 \times\{\sum_f|\langle i|M|f\rangle|^2\delta(E_i-E_f)\delta^3(\mathbf{P}_i-\mathbf{P}_f)\}_{\mathrm{av}\,i}, \quad (4.1)$$

where we sum over final states and average over initial states. The amplitude $\langle i|M|f\rangle$ is related to the S matrix element by

$$\langle f|S|i\rangle=(2\pi\hbar)^4\delta(E_i-E_f)\delta^3(\mathbf{P}_i-\mathbf{P}_f)\langle f|M|i\rangle. \quad (4.2)$$

The volume V_0 that must be considered for this problem is the actual volume of interaction of the laser beams in the plasma.

The density of final states for this problem is

$$\rho(E_f)=\int\frac{d^3k_3}{(2\pi)^3}\frac{d^3k_4}{(2\pi)^3}(2\pi)^4V_0^2 \times\delta^3(\mathbf{k}_1+\mathbf{k}_2-\mathbf{k}_3-\mathbf{k}_4)\delta(\omega_1+\omega_2-\omega_3-\omega_4). \quad (4.3)$$

If we observe only one of the scattered photons, say, $\mathbf{k}_3$ for some particular small range of values, then we integrate over $\mathbf{k}_4$ and we find

$$\rho(E_f)=\left(\frac{V_0}{2\pi}\right)^2\frac{d\Omega_3}{c^3}\frac{\omega_3^2}{1-\cos2\theta'}, \quad (4.4)$$

where

$$\cos2\theta'=\hat{k}_3\cdot\hat{k}_4. \quad (4.5)$$

Consider the symmetric case in which $\omega_1=\omega_2=\omega_0$. Then the total momentum of the incoming radiation defines an axis of symmetry. The final wave vector $\mathbf{k}_3$ is restricted by conservation of energy and momentum to lie in a cone of angle θ_3 from the axis of symmetry where

$$\cos\theta_3=\frac{\cos2\theta_0+1+2(\omega/\omega_0)}{2\cos\theta_0(1+\omega/\omega_0)}, \quad (4.6)$$

where $\omega=\omega_3-\omega_1=\omega_3-\omega_0$ and $\cos2\theta_0=\hat{k}_1\cdot\hat{k}_2$. In the case $\omega/\omega_0\ll1$, for which our approximations are valid, we see that

$$\theta_3=\theta_0, \quad (4.7)$$

to terms of order ω/ω_0. The scattered radiation thus is found in a cone of angle θ_0 which subtends a solid angle

$$\Delta\Omega_3=2\pi(\Delta\omega/\omega_0)(\sin^2\theta_0/\cos\theta_0), \quad (4.8)$$

where $\Delta\omega$ is the effective range of frequency shifts of the scattered radiation. We shall see that $\Delta\omega/\omega_0\ll1$ when collective effects are taken into account so that the scattered radiation is confined to a very thin cone.

If we use (4.2), (4.4), and (2.8), we obtain for the differential scattering rate into $d\Omega_3$

$$\frac{d\Gamma}{d\Omega_3}=\frac{r_0^2}{4m^2}\frac{n_1n_2c}{V_0}\frac{1}{\omega_1\omega_2}\frac{\omega_3}{\omega_4}\frac{1}{1-\cos2\theta'} \times|(4\pi e^2)e_1^\mu e_2^\nu e_3^\sigma e_4^\rho G_{\mu\nu\sigma\rho}(k_1,k_2,k_3,k_4)|^2, \quad (4.9)$$

where $\mathbf{k}_1$, $\mathbf{k}_2$; $\mathbf{k}_3$, $\mathbf{k}_4$ and ω_1, ω_2, ω_3, ω_4 are restricted by conservation of energy and momentum. For ω_1, $\omega_2\gg\omega_p$ we have seen that the first term in (2.9) for $G_{\mu\nu\sigma\rho}$ [Fig. 1(a)], which transfers an energy $\omega_1+\omega_2$ to the density fluctuation, is negligible compared to the other terms which transfer an energy $\omega_1-\omega_3$, $\omega_1-\omega_4$ provided these differences are small. Keeping only these amplitudes, using (2.9), (2.13), and (4.9) we have

$$\frac{d\Gamma}{d\Omega_3}=r_0^2\frac{n_1n_2c}{V_0}\left(\frac{\omega_p}{\omega_0}\right)^2\frac{1}{1-\cos2\theta'} \times\left(\frac{\omega_p^2}{\omega}\right)[1-(\hat{e}_1\cdot\hat{k}_3)^2][1-(\hat{e}_1\cdot\hat{k}_4)^2] \cdot\left(\frac{4\pi e^2}{k_D^2}\right)^2\left|\mathrm{Im}\Pi_{ee}^+(\mathbf{k},\omega)+\mathrm{Im}\Pi_{ee}^+(\mathbf{k}',\omega)\right|^2. \quad (4.10)$$

Here we have also chosen the symmetric case $\omega_1=\omega_2=\omega_0$ and $\hat{e}_1=\hat{e}_2$ and have summed over outgoing polarizations $\hat{e}_3$ and $\hat{e}_4$.

If the scattered radiation is observed in the plane perpendicular to that of the incoming radiation, then $k\simeq k'=\sqrt{2}k_0\sin\theta_0$. In Fig. 2 we plot the frequency distribution of the scattered light

$$\frac{d\Gamma}{d\omega}=\frac{d\Gamma}{d\Omega_3}\frac{2\pi}{\omega_0}\frac{\sin^2\theta_0}{\cos\theta_0}, \tag{4.11}$$

as a function of ω in the RPA using (2.14). This rate being proportional to $\omega^{-2}|\mathrm{Im}\Pi_{ee}(k,\omega)|^2$ is proportional to the square of the rate or cross section for incoherent scattering.[3] For $k\ll k_D$ the spectrum is dominated by a central line of width approximately given by

$$\Delta\omega\simeq\left(\frac{m_e}{m_i}\right)^{1/2}\frac{k}{k_D}\omega_p=k\left(\frac{kT}{m_i}\right)^{1/2}, \tag{4.12}$$

which arises from the low-frequency ion acoustic plasma resonance. At $\omega=\pm\omega_p$ there is also a resonance but in this experiment it is weaker than the central line by a factor of $(k/k_D)^4$. A more detailed discussion of the behavior of $\mathrm{Im}\Pi_{ee}^{+}(k,\omega)$ including the effect of collisions is given in Ref. 3.

The total scattering rate integrated over the central resonance can be obtained by integrating

$$\int_{-\infty}^{\infty}d\omega\left|\frac{\mathrm{Im}\Pi_{ee}^{+}(k,\omega)}{\omega}\right|^2. \tag{4.13}$$

Using only the second term in (2.14) which is the only contribution near the central line

$$\frac{\pi}{2}\int_{-\infty}^{\infty}d\omega\frac{1}{\alpha^2k^2}e^{-(\omega/\alpha k)^2}\left|\frac{Q_0(\omega/k)}{k^2+Q_0(\omega/k)+Q_0(\omega/\alpha k)}\right|^4. \tag{4.14}$$

Changing variables to $z=\omega/\alpha k$, this becomes

$$\frac{\pi}{2\alpha k}\int_{-\infty}^{\infty}dze^{-z}\cdot\left|\frac{1}{k^2+1+Q_0(z)}\right|^4\simeq\frac{0.3\pi}{2\alpha k}, \tag{4.15}$$

using $\lim_{\alpha\to 0}Q(\alpha z)=1$ and $k\ll 1$ to carry out a numerical integration. This integral becomes anomalously large as $\alpha k\to 0$ because of the very large contribution from small ω in the collisionless approximation for $\Pi_{ee}(\mathbf{k},\omega)$. The collisionless approximation, however, is valid only for $\omega\gg\Gamma_{ee}$, where Γ_{ee} is the electron-electron collision frequency.[3] To take this into account we can cut off the ω integral at a lower limit of Γ_{ee} and we find that (4.15) is valid to terms of order $(\Gamma_{ee}/\alpha k)$. Therefore (in ordinary units) if

$$\alpha(k/k_D)\omega_p\gg\Gamma_{ee}\sim\omega_p\lambda\ln(\lambda^{-1}), \tag{4.16}$$

then (4.15) can be used.

The total rate over the central line is then roughly [using $\alpha=(m/M)^{1/2}$] for photons scattered in a plane perpendicular to the incoming light

$$\Gamma_{\mathrm{Tot.}}\simeq\frac{0.3r_0^2}{2}\pi^2\frac{n_1n_2c}{V_0}\left(\frac{M}{m}\right)^{1/2}\left(\frac{\omega_p}{\omega_0}\right)^3\left(\frac{k_p}{k}\right)\cos^3\theta_0$$

$$\simeq 10^{-11}\frac{n_1n_2c}{V_0}\left(\frac{M}{m}\right)^{1/2}\frac{1}{\omega_0^3}\frac{1}{k}\frac{n^2}{T^{1/2}}. \tag{4.17}$$

These photons are confined to a solid angle

$$\Delta\Omega_3=\Delta\phi\frac{\Delta\omega}{\omega_0}\frac{\sin^2\theta_0}{\cos\theta_0}=\Delta\phi\left(\frac{m}{M}\right)^{1/2}\frac{k}{k_D}\frac{\omega_p}{\omega_0}\frac{\sin^2\theta_0}{\cos\theta_0}, \tag{4.18}$$

where we have used (4.8) and (4.12). Here $\Delta\phi$ is the increment of azmuthal angle subtended by the detector. This formula applies to a well collimated beam in which the angular divergence of the beam is much smaller than $\Delta\Omega_3$ a situation which is easily obtainable from a laser.[9]

Including (4.16) we have placed the following restrictions for the validity of (3.17): (i) $\omega_0=\omega_1=\omega_2\gg\omega_p$ so that the $\mathbf{j}\cdot\mathbf{A}$ interactions can be dropped; (ii) $k_1=k_2\ll k_D$ so that collective effects dominate and the principal scattering is confined to the narrow central line. (iii) $\lambda=k_0^3/n\ll 1$ so that we have a weakly coupled plasma and (iv) $\alpha(k/k_D)\gg\lambda\ln(1/\lambda)$ as in (4.16).

---

[9] Because of the smallness of the solid angle $\Delta\Omega$ into which the light is scattered for a well collimated beam, the competing background of incoherent scattering can be greatly reduced. The differential scattering rate $d^2\Gamma/d\omega_3d\Omega_3$ for incoherent scattering integrated over the frequency range of the central ion resonance is (see Ref. 3)

$$\frac{d\Gamma}{d\Omega_3}=\frac{n_1cN}{V_0}r_0^2\tfrac{1}{2}[1+(\hat{k}_1\cdot\hat{k}_3)^2]\simeq\frac{n_1cN}{V_0}r_1^2,$$

where N is the total number of electrons illuminated by the beam. Note that this rate is proportional to the solid angle $d\Omega_3$ in which the scattered photon is observed. If we take this solid angle to be $\Delta\Omega_3$ of Eq. (4.18) which contains the entire central line in the light by light scattering, we find the ratio of the scattering rates

$$\frac{\Gamma_{\mathrm{tot}}(\text{light by light})}{\Gamma(\text{incoherent})}\simeq\frac{1.2\pi^2}{\sqrt{2}}\Delta\phi\frac{n_2}{N}\frac{M}{m}\left(\frac{\omega_p}{\omega_0}\right)^2\left(\frac{k_D}{k}\right)^2.$$

The factor n_2/N can be made at least of order unity using a ruby giant pulse laser and $N\sim 10^{17}$. The factor $(M/m)(k_D/k)^2$ can easily be made large enough to overcome the small factor $(\omega_p/\omega_0)^2$. Therefore, this ratio can be made greater than unity. This feature of the experiment makes it possible to discriminate against the background of competing processes. In addition, since this is a two-beam experiment, coincidence techniques can be used to discriminate against background. This feature has also been pointed out by Platzman, Buchsbaum, and Tzoar (to be published) who consequently believe that even the weaker plasma line can be observed in light by light scattering. The formula for the scattering rate at the electron plasma resonance is obtained from our general results (4.9), (2.9), and (2.13), by noting (see Ref. 3) that if $kv_e\ll\omega$, then $4\pi e^2\,\mathrm{Im}\Pi_{ee}^{+}(k,\omega)=k^2\,\mathrm{Im}[\epsilon_L^{+}(k,\omega)]^{-1}$. This approximation, however, is not valid near the ion resonances. The authors are indebted to Dr. P. M. Platzman for communicating these results to us prior to publication.

Under these conditions, a rather high plasma density and temperature are required to achieve an observable counting rate using existing laser technology. For example, using an amplified giant pulse ruby laser, it is possible to obtain $n_1=n_2=10^{16}$ photons in an interaction volume $V^0=10^{-1}$ cm^3 with $k_1=10^5$ cm^{-1}, $\omega_0=3\times10^{15}$ sec^{-1}. To achieve a counting rate of 10^{14} photons per second or 10^6 photons in a 10^{-8} second laser pulse requires [with $(M/m)^{1/2}=10^2$] (T in °K)

$$n^2/T^{1/2}\gtrsim10^{30}. \tag{4.19}$$

This restriction as well as those listed above can be met for the minimum values $n\simeq3\times10^{17}$ cm^{-3} and $T\simeq2\times10^5$ °K$=20$ eV. Such plasmas are probably obtainable in various magnetic pinch machines.[10]

ACKNOWLEDGMENTS

The authors wish to thank Dr. W. Wagner and Dr. R. W. Hellwarth for several helpful discussions.

[10] The main restriction involved in the above estimate is the requirement $k_1\ll k_D$ which requires $n/T<10^{12}$ if $k_1=10^5$ cm^{-1}. However, if the experiment could be performed at extremely small scattering angles θ then we have $k=k_1\theta$ and we can relax the condition $k_1<k_D$. In this case the principal limitations are $\alpha(k/k_D)\gg\lambda\ln\lambda^{-1}$ and the requirement (4.19) on the counting rate. These conditions can be satisfied for the minimal values $n\sim10^{16}$ cm^{-3} and $T\sim3$ eV. For forward angles, however, the problems of background discrimination would become more difficult.

PHYSICAL REVIEW VOLUME 135, NUMBER 4A 17 AUGUST 1964

Mobility of Positive Ions in Liquefied Argon and Nitrogen*

BOB L. HENSON

Department of Physics, Washington University, St. Louis, Missouri

(Received 19 March 1964)

Drift velocities of positive ions in liquid argon and liquid nitrogen have been measured for applied electric fields in the range from 0 to 4300 V/cm. These data were taken at pressures of 1 atm and at temperatures corresponding to the respective liquids' boiling points at this pressure. A time-of-flight spectrometer, consisting of an ion source, an electronic shutter, and a final drift space, was used. The ions were produced by the technique of field ionization. This was accomplished by immersing a tungsten point (etched down to a radius of less than 1000 Å) in the respective liquefied gases and applying a high potential to it. The times of flight of the ions across the final drift space were determined by amplifying the ion current and displaying it on an oscilloscope. It was found that step-like changes in the curves of ion mobility versus E occurred in both liquid argon and liquid nitrogen. Five such constant-mobility regions were found in liquid argon and four in liquid nitrogen. These constant mobilities were found to be 6.0×10^{-4}, 9.75×10^{-4}, 8.50×10^{-4}, 7.75×10^{-4}, and 7.25×10^{-4} cm^2/V-sec in liquid argon, and 2.50×10^{-3}, 1.80×10^{-3}, 1.54×10^{-3}, and 1.36×10^{-3} cm^2/V-sec in liquid nitrogen. It is suggested that these mobilities may correspond to ionic clusters.

I. INTRODUCTION

PARTICULARLY during the past 12 years, the measurement of mobility of ions in gases has been developed as a powerful tool for the identification of the ions. Enough cross comparisons with mass spectrographic data have been made to establish the validity of mobility measurements for such identification. The existence of several types of ion in one gas, for example, He^+ and He_2^+ in helium,[1] and the change of one ion to another with changing field strength to pressure ratio, E/p, as for example, N_2^+ changing to N_4^+,[2] are illustrations of the successes of mobility measurements in accomplishing ion-type identification.

In gases, the cross section for ion-molecule collisions regulating the mobility is a momentum transfer cross section. There are at least three different atomic phenomena now well known which contribute to this cross section. The first and most obvious is the hard-sphere cross section. While the actual form of interaction is probably an inverse ninth power repulsive force, a hard-sphere model is a good approximation. The second critical atomic characteristic influencing momentum transfer cross sections is the inverse fifth power attractive polarization force acting on ions in the vicinity of atoms or molecules. (In this work, only nonpolar substances are contemplated so that atomic or molecular polarizations must be induced by the field of the ions in the near proximity.) The combination of these two forces was assembled into a single theory of mobilities by Langevin[3] in 1905 in a monumental work both in point of effort and importance. In it, by laborious numerical integrations, he deduced equivalent momentum transfer cross sections. Quantum-mechanical modernizations by Hassé and Cook[4] in the period 1926 to 1931 have improved but only slightly altered Langevin's results.

The third atomic phenomenon of key influence on

* Work supported by a grant DA-ARO-D-31-124-G432.

[1] J. A. Hornbeck, Phys. Rev. **83**, 374 (1951); **84**, 615 (1952).

[2] R. N. Varney, Phys. Rev. **89**, 708 (1953).

[3] P. Langevin, Ann. Chim. et Phys. **8**, 245 (1905).

[4] H. R. Hassé and W. R. Cook, Phil. Mag. **12**, 554 (1931).